Supplementary material
A Bispectral 3D U-Net for Rotation Robustness Segmentation in Medical Segmentation

1 Segmentation Visualisation

Comparison of the segmentation performances of the different model's output. Only the positive class prediction is shown. The colour represents the model's softmax output, i.e. a score of 1 is perfect confidence whereas a score of 0.5 is the worst as a lower score leads to background prediction.

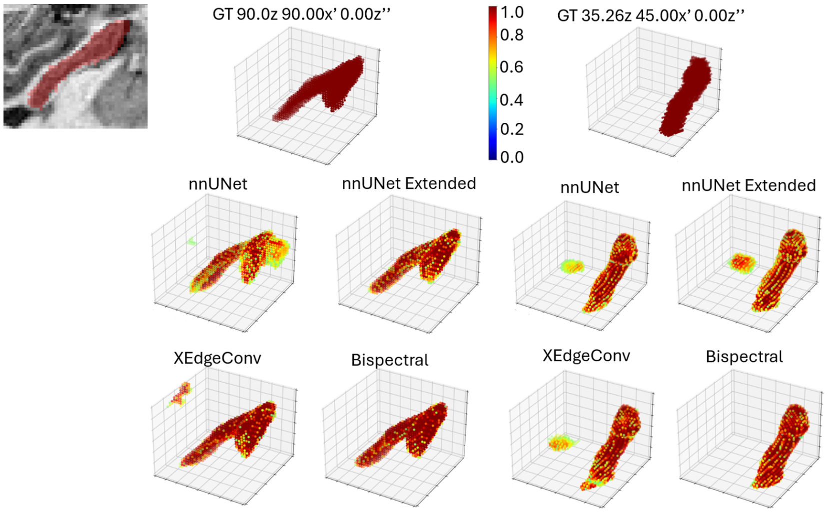

Figure 1: Prediction confidence of each model for a right-angle rotation, left side, and a cone rotation, right side, of the HC dataset. Only hippocampus prediction is kept and background prediction is not shown. A slice of the input volume is shown in the top left corner.

2 Equivariance properties of the bispectral layer

This supplementary material aims to demonstrate the equivariance to translations and rotations of the proposed operator $\mathcal{G}^{o}_{n,n',l}$ used in each layer of the proposed Bispectral U-Net (see Section 3.3). Note that this cannot be deduced by known results since this vector depends on all the input images $y_{1\leq i\leq C_{in}}$ of the layer. We shall rely on the work of Kakarala and Mao [1], where more details are provided regarding the properties of Wigner matrices and the representation theoretic framework behind the algebraic properties.

We recall some notations in addition to the ones introduced in Section 3.1. A block diagonal matrix formed by the sub-matrices A_i is written as $[\bigoplus_i \mathrm{A}_i]$.

For any spherical Fourier vectors $\boldsymbol{\mathcal{F}}_n$, $\boldsymbol{\mathcal{H}}_{n'}$, and $\boldsymbol{\mathcal{Q}}_l$ of adequate sizes and possibly different spherical functions, we introduce the operator $\mathcal{B}$ as

$$\mathcal{B}\{\boldsymbol{\mathcal{F}}_n, \boldsymbol{\mathcal{H}}_{n'}, \boldsymbol{\mathcal{Q}}_l\} = [\boldsymbol{\mathcal{F}}_n \otimes \boldsymbol{\mathcal{H}}_{n'}] C_{nn'} \tilde{\boldsymbol{\mathcal{Q}}_l}^{\dagger}. \tag{1}$$

We observe that when the Fourier vectors comes from the same spherical function f, we recover the bispectrum $\mathcal{B}\{\boldsymbol{\mathcal{F}}_n, \boldsymbol{\mathcal{F}}_{n'}, \boldsymbol{\mathcal{F}}_l\} = b^{l}_{n,n'}(f)$ (see Eq. (3) in the paper). First, we prove the following lemma.

Lemma 1. *The bispectrum operator $\mathcal{B}$ is invariant to multiplication of its arguments by Wigner matrices associated with the same rotation. This means that, for any rotation $\mathrm{R}_0 \in SO(3)$ and any spherical Fourier vectors $\boldsymbol{\mathcal{F}}_n$, $\boldsymbol{\mathcal{H}}_{n'}$, $\boldsymbol{\mathcal{Q}}_l$ we have*

$$\mathcal{B}\{\boldsymbol{\mathcal{F}}_n \mathrm{D}_n(\mathrm{R}_0), \boldsymbol{\mathcal{H}}_{n'} \mathrm{D}_{n'}(\mathrm{R}_0), \boldsymbol{\mathcal{Q}}_l \mathrm{D}_l(\mathrm{R}_0)\} = \mathcal{B}\{\boldsymbol{\mathcal{F}}_n, \boldsymbol{\mathcal{H}}_{n'}, \boldsymbol{\mathcal{Q}}_l\}. \tag{2}$$

Proof. We first observe that the respective Fourier vectors $\boldsymbol{\mathcal{F}}_n$ and $\boldsymbol{\mathcal{F}}'_n$ of $f \in L_2(\mathbb{S}^2)$ and its rotated version $f(\mathrm{R}_0 \cdot)$ with $\mathrm{R}_0 \in SO(3)$ satisfy [1, Section 3 Eq. (5)]

$$\boldsymbol{\mathcal{F}}'_n = \boldsymbol{\mathcal{F}}_n \mathrm{D}_n(\mathrm{R}_0). \tag{3}$$

For a spherical Fourier vector $\boldsymbol{\mathcal{Q}}_\ell$, its rotated version $\boldsymbol{\mathcal{Q}}'_\ell = \boldsymbol{\mathcal{Q}}_\ell \mathrm{D}_\ell(\mathrm{R}_0)$ can be embedded as [1, Section 4, Eq. 30]

$$\widetilde{\boldsymbol{\mathcal{Q}}'}_\ell = \widetilde{\boldsymbol{\mathcal{Q}}}_\ell \left[\bigoplus_{\ell=|n-n'|}^{n+n'} \mathrm{D}_\ell(\mathrm{R}_0)\right]. \tag{4}$$

Now, considering the action of $\mathcal{B}$ on rotated arguments, we have

$$\begin{aligned}
\mathcal{B}\{\boldsymbol{\mathcal{F}}_n \mathrm{D}_n(\mathrm{R}_0), \boldsymbol{\mathcal{H}}_{n'} \mathrm{D}_{n'}(\mathrm{R}_0), \boldsymbol{\mathcal{Q}}_l \mathrm{D}_l(\mathrm{R}_0)\} &= [\boldsymbol{\mathcal{F}}_n \mathrm{D}_n(\mathrm{R}_0) \otimes \boldsymbol{\mathcal{H}}_{n'} \mathrm{D}_{n'}(\mathrm{R}_0)] \mathrm{C}_{nn'} \widetilde{\boldsymbol{\mathcal{Q}}'}_\ell^{\dagger} \\
&= [\boldsymbol{\mathcal{F}}_n \mathrm{D}_n(\mathrm{R}_0) \otimes \boldsymbol{\mathcal{H}}_{n'} \mathrm{D}_{n'}(\mathrm{R}_0)] \mathrm{C}_{nn'} \left[\bigoplus_{\ell=|n-n'|}^{n+n'} \mathrm{D}_\ell(\mathrm{R}_0)^{\dagger}\right] \widetilde{\boldsymbol{\mathcal{Q}}}_\ell^{\dagger} \\
&= [\boldsymbol{\mathcal{F}}_n \otimes \boldsymbol{\mathcal{H}}_{n'}] \left\{ [\mathrm{D}(\mathrm{R}_0)_n \otimes \mathrm{D}_{n'}(\mathrm{R}_0)] \mathrm{C}_{nn'} \left[\bigoplus_{\ell=|n-n'|}^{n+n'} \mathrm{D}_\ell(\mathrm{R}_0)^{\dagger}\right] \right\} \widetilde{\boldsymbol{\mathcal{Q}}}_\ell^{\dagger}.
\end{aligned}$$

By [1, Section 3, Eq. (19)] and the unitary property of the Wigner matrices and Clebsch-Gordan matrices, the content of the bracket simplifies to the Clebsch-Gordan matrix $\mathrm{C}_{nn'}$, confirming the validity of Lemma 1. $\square$

We consider the feature maps computed at the considered layer

$$\mathcal{G}^{o}_{n,n',\ell}\{\boldsymbol{y}\}(\boldsymbol{x}) = \mathcal{B}\{\boldsymbol{\mathcal{F}}^{o}_{n}(\boldsymbol{x}), \boldsymbol{\mathcal{F}}^{o}_{n'}(\boldsymbol{x}), \boldsymbol{\mathcal{F}}^{o}_{\ell}(\boldsymbol{x})\}, \tag{5}$$

with $\boldsymbol{y}(\boldsymbol{x}) = [y_1(\boldsymbol{x}), \dots, y_{C_{in}}(\boldsymbol{x})]$ and $\boldsymbol{\mathcal{F}}^{o}_{n}(\boldsymbol{x}) = \sum_{i=1}^{C_{in}}[(y_i * \kappa^{i,o}_{n,m})(\boldsymbol{x})]^{m=n}_{m=-n}$ as defined in Eq. (8) in the paper. Without loss of generality, we omit the o index for clarity. By the definition of the Wigner matrices and the steerability properties of the SH, we have $Y_n^m(\mathrm{R}_0\cdot) = \sum_{m'=-n}^{n}[\mathrm{D}_n(\mathrm{R}_0)]_{m',m}Y_n^{m'}$. This relation applied to $\mathrm{R} = \mathrm{R}_0^{-1}$, we have that

$$\kappa_{n,m}(\mathrm{R}_0^{-1}\cdot) = \sum_{m'=-n}^{n} \mathrm{D}_n(\mathrm{R}_0^{-1})_{m,m'}\kappa_{n,m}. \tag{6}$$

Let $\boldsymbol{\mathcal{F}}_n(\boldsymbol{x})$ and $\boldsymbol{\mathcal{F}}'_n(\boldsymbol{x})$ be the Fourier feature maps of $\boldsymbol{y}$ and $\boldsymbol{y}(\mathrm{R}_0\cdot)$ respectively, with $\mathrm{R}_0 \in SO(3)$. Moreover, we have that $(y_i(\mathrm{R}_0\cdot) * \kappa^{i}_{n,m})(\boldsymbol{x}) = (y_i * \kappa^{i}_{n,m}(\mathrm{R}_0^{-1}\cdot))(\mathrm{R}_0\boldsymbol{x})$. Together with (6), this implies that

$$\boldsymbol{\mathcal{F}}'_n(\boldsymbol{x}) = \sum_{i=1}^{C_{in}}[(y_i(\mathrm{R}_0\cdot) * \kappa^{i}_{n,m})(\boldsymbol{x})]^{m=n}_{m=-n} = \boldsymbol{\mathcal{F}}_n(\mathrm{R}_0\boldsymbol{x})\mathrm{D}_n(\mathrm{R}_0^{-1}). \tag{7}$$

Eq. (7) together with Lemma 1 demonstrates the equivariance to rotations of the proposed layer:

$$\begin{aligned}
\mathcal{G}_{n,n',\ell}\{\boldsymbol{y}(\mathrm{R}_0\cdot)\}(\boldsymbol{x}) &= \mathcal{B}\{\boldsymbol{\mathcal{F}}'_n(\boldsymbol{x}), \boldsymbol{\mathcal{F}}'_{n'}(\boldsymbol{x}), \boldsymbol{\mathcal{F}}'_{\ell}(\boldsymbol{x})\} \\
&= \mathcal{B}\{\boldsymbol{\mathcal{F}}_n(\mathrm{R}_0\boldsymbol{x})\mathrm{D}_n(\mathrm{R}_0^{-1}), \boldsymbol{\mathcal{F}}_{n'}(\mathrm{R}_0\boldsymbol{x})\mathrm{D}_{n'}(\mathrm{R}_0^{-1}), \boldsymbol{\mathcal{F}}_{\ell}(\mathrm{R}_0\boldsymbol{x})\mathrm{D}_{\ell}(\mathrm{R}_0^{-1})\} \\
&= \mathcal{B}\{\boldsymbol{\mathcal{F}}_n(\mathrm{R}_0\boldsymbol{x}), \boldsymbol{\mathcal{F}}_{n'}(\mathrm{R}_0\boldsymbol{x}), \boldsymbol{\mathcal{F}}_{\ell}(\mathrm{R}_0\boldsymbol{x})\} \\
&= \mathcal{G}_{n,n',\ell}\{\boldsymbol{y}\}(\mathrm{R}_0\boldsymbol{x}),
\end{aligned}$$

References

[1] Kakarala, R., Mao, D.: A theory of phase-sensitive rotation invariance with spherical harmonic and moment-based representations. In: Computer Vision and Pattern Recognition (CVPR), 2010 IEEE Conference on. pp. 105–112. IEEE (2010)